

Equation Sheet

Serena Patel, Dharik Mallapragada

February 8, 2024

1 Nomenclature and Data Inputs

The section below describes the nomenclature used in both model formulations as well as the data inputs. All economic parameters are converted from their respective sources to 2020 USD using either the Consumer Price Index (CPI) or the Chemical Engineering Plant Cost Index (CEPCI) when appropriate.

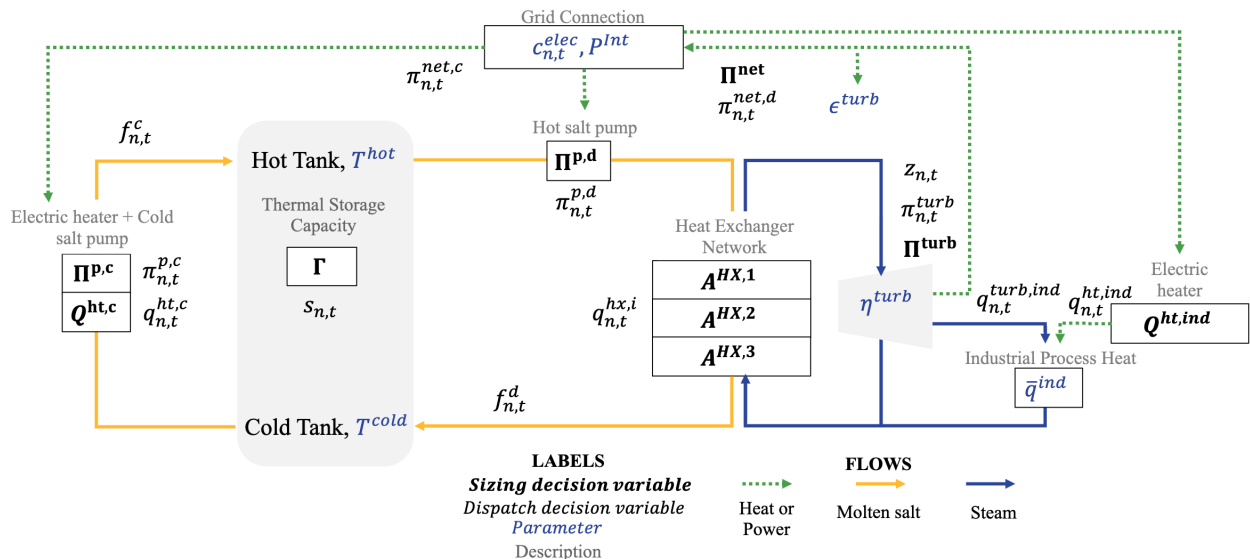


Figure S1: Diagram describing the decision variables and some parameters in the integrated sizing and dispatch optimization model.

Set	Description
$t \in T$	Set of time periods in each week ranging from 1 to t_{end} (i.e. 168)
$n \in N$	Set of representative weeks modeled ranging from 1 to n_{end} (i.e. 23)
$w \in W$	Set of weeks over the years ranging from 1 to w_{end} (i.e. 52)
$i \in I = ec, ev, su$	Set of heat exchangers modeled
$g \in G = solar, wind, coal$	Set of generators
$g \in G^{VRE} = solar, wind$	Set of variable renewable generators

Table S1: Sets and Indices

Variable	Description
Γ	Installed energy storage capacity ($MWh_{thermal}$)
Γ^b	Installed energy storage capacity of Li-ion battery b (MWh)
$\Pi^{p,d}, \Pi^{p,c}$	Size of salt pumps for discharging and charging, respectively (MW)
Π^{turb}	Peak capacity of steam cycle (MW)
Π^g	Peak capacity of generator g (MW)
Π^b	Peak capacity of Li-ion battery b (MW)
$Q^{ht, TES}, Q^{ht, IND}$	peak charging thermal power capacity for heating molten salt and heater used to provide industrial process heat ($MW_{thermal}$)
$A^{HX,i}$	areas of three heat exchanger $i \in I$ (economizer, evaporator, and superheater part of the heat exchanger network)
$\lambda_k^{ec}, \lambda_k^{ev}, \lambda_k^{su}$	SOS variables of type 2 to model piece-wise linear approximation of capital costs for heat exchanger $i \in I$
$C^{HX,i}$	Capital cost of heat exchanger $i \in I$

Table S2: Time-independent Variables

Variable	Description
$q_{n,t}^{hx,i}$	Rate of heat exchanged via heat exchanger $i \in I$ during subperiod t of representative week n ($MW_{thermal}$)
$q_{n,t}^{ht,c}, q_{n,t}^{ht,ind}$	Heat supplied by resistive heater during for heating up salt and providing industrial process heat, respectively, during sub-period t of representative week n ($MW_{thermal}$)
$q_{n,t}^{turb,ind}$	Heat supplied by steam to meet industrial process heat, respectively, during sub-period t of representative week n ($MW_{thermal}$)
$f_{n,t}^c, f_{n,t}^d$	Flow rate of salt for charging and discharging during sub-period t of representative week n (tonne per s)
$\gamma_{n,t}$	TES storage inventory for during sub-period t of representative week n ($MW_{thermal}$)
$\gamma_{n,t}^b$	Li-ion battery storage inventory for during sub-period t of representative week n (MW)
$\pi_{n,t}^g$	generation in sub-period t of representative week n (MW) for generator g
$\pi_{n,t}^{b,c}, \pi_{n,t}^{b,d}$	Li-ion battery, b , charging (c) and discharging (d) in sub-period t of representative week n (MW)
s_w	TES storage inventory at the beginning of week $w \in W$ ($MWh_{thermal}$)
δ_n	Change in energy storage inventory over the course of representative week n ($MWh_{thermal}$)
$y_{n,t}^{TES}, y_{n,t}^{coal}$	Binary variable tracking whether steam turbine system is in discharging (=1) or charging mode (=0) during sub-period t of representative week n for TES and coal
$z_{n,t}^{TES}, z_{n,t}^{coal}$	Binary variable used track start-up of steam cycle during sub-period t of representative week n for TES and coal

Table S3: Time-dependent Variables

Variable	Parameter	Value
M	Big M parameter	6000
$\lambda^a, \lambda^b, \lambda^c$	Special Ordered Set Type 1 for heat exchanger a,b,c	-
k	Increment for piece-wise linearization of cost function for heat exchangers	0.1
m_n	Weight of each representative week n	-

Table S4: Modeling Parameters

Symbol	Parameter	Value	Source
c^{TES}	Storage cost (\$/ kWh_t)	20.89	See S.I. Table S8
$c^{ht,c}$	Charger cost (\$/ kW_t)	3.3	[16]
$c^{ht,ind}$	Heater cost (\$/ kW_t)	3.3	[16]
c^{pipes}	Pipes and valves cost (\$/ kW_e)	4.66	[10]
c^{start}	Start up-cost (\$/ MW)	10.15	[18], [13], [4]
$\bar{n}^{HX,ec}$	Exponent describing relationship of economizer size and cost	0.684	Table 11 from [8]
$\bar{n}^{HX,ev}$	Exponent describing relationship of evaporator size and cost	0.788	Table 11 from [8]
$\bar{n}^{HX,su}$	Exponent describing relationship of superheater size and cost	0.741	Table 11 from [8]
$\bar{C}^{HX,ec}$	Economizer base cost associated with $\bar{A}^{HX,ec}(\$)$	2,225,472	[8]
$\bar{C}^{HX,ev}$	Evaporator base cost associated with $\bar{A}^{HX,ev}(\$)$	2,752,992	[8]
$\bar{C}^{HX,su}$	Superheater base cost associated with $\bar{A}^{HX,su}(\$)$	434,693	[8]
U^{ec}	Economizer heat exchange coefficient (kW/m^2K)	1.448	Table 4 from [12]
U^{ev}	Evaporator heat exchange coefficient (kW/m^2K)	1.295	Table 4 from [12]
U^{su}	Superheater heat exchange coefficient (kW/m^2K)	1.241	Table 4 from [12]
$\bar{A}^{HX,ec}$	Economizer base area (m^2)	10,000	Table 11, 12 from [8]
$\bar{A}^{HX,ev}$	Evaporator base area (m^2)	5000	Table 11, 12 from [8]
$\bar{A}^{HX,su}$	Superheater base area (m^2)	505	Table 11, 12 from [8]
R	Annual real discount rate.	0.09	[7]
L^{REM}	Remaining lifetime, used for the retrofitted system (yrs)	25	[19]
$c_{n,t}^{elec}$	Marginal cost of electricity at time t in representative week n	-	[5]
$d_{n,t}$	Electricity demand at time t in representative week n	-	[2]
$FOM_{turbine}$	Fixed Operational & Maintenance Cost of TES turbine (\$/ $kW/year$)	13.5	

Table S5: Economic Parameters

Symbol	Parameter	Value	Source
FOM^{coal}	Fixed Operational & Maintenance Cost of coal plant (\$/kW/year)	31.248	[1]
FOM^{solar}	Fixed Operational & Maintenance Cost of solar installations (\$/kW/year)	2.644	[1]
FOM^{wind}	Fixed Operational & Maintenance Cost of wind installations (\$/kW/year)	7.691	[1]
FOM^b	Fixed Operational & Maintenance Cost of Li-ion battery (\$/kW/year)	6.009	[1]
$c^{solar,inv}$	Investment cost for solar (\$/kW)	46.355	[1]
$c^{wind,inv}$	Investment cost for wind (\$/kW)	72.99	[1]
$c^{p,inv}$	Investment cost for Li-ion battery power capacity (\$/kW)	48.89	[1]
$c^{e,inv}$	Investment cost for Li-ion battery energy capacity (\$/kWh)	17.3089	[1]
$OPEX^{solar}$	Operational cost of solar (\$/kWh)	0	[1]
$OPEX^{wind}$	Operational cost of wind (\$/kWh)	0.0027	[1]
$OPEX^{coal}$	Operational cost of coal (\$/kWh)	0.145	[1]
$OPEX^{dis}$	Operational cost of Li-ion battery dispatch (\$/kWh)	0.0001	[1]
$OPEX^{ch}$	Operational cost of Li-ion battery charge (\$/kWh)	0.001	[1]

Table S6: Additional Economic Parameters for CEM

Symbol	Parameter	Value	Source
C_p	Specific heat capacity (kJ/kgK)	1.56	[19], [3]
β^{min}	Minimum Power Fraction	0.17	[15]
η^{ht}	Charging efficiency for TES (%)	0.95	[16]
$\eta^{b,c}, \eta^{b,d}$	Charging (c) and discharging (d) efficiency for Li-ion battery (%)	0.95	[16]
η^{pump}	Pump efficiency (%)	0.75	[21]
G	Gravitational constant (m/s^2)	9.81	-
H	Pump head (m)	15	[21]
ϵ^{sd}	Hourly self-discharge rate (%/hr)	0.000416667	[11]
ϵ^b	Hourly self-discharge rate for Li-ion battery (%/hr)	0	-
$\epsilon^{sd,wk}$	Weekly self-discharge rate (%/week)	7	[11]
P^{Int}	Interconnection power limit (MW_e)	500	Base Case
$\beta^{ramp,i}$	Ramp Rate, $i \in \{up, dn\}$ (%/hr)	50	[9]
η^{turb}	Steam turbine cycle efficiency (%)	0.41	Base Case
q^{ind}	Constant industrial process heat demand (MW)	-	-
$\bar{\alpha}^c, \bar{\beta}^c$	Coefficients describing relationship between cold salt pump power consumption cost	200.56, 475	[11]
$\bar{\alpha}^d, \bar{\beta}^d$	Coefficients describing relationship between hot salt pump power consumption cost	154.73, 1433.9	[11]
$\Delta T^{LM,su}$	Log mean temperature difference of the superheater	66.57	Base Case
$\Delta T^{LM,ec}$	Log mean temperature difference of the economizer	145.5	Base Case
$\Delta T^{LM,ev}$	Log mean temperature difference of the evaporator	102.64	Base Case
ΔT^{salt}	Molten salt temperature difference	277	[19], [3]
Π^{turb}	Maximum capacity of steam cycle (MW)	-	-
β^{coal}	Emission Rate of coal power plant (tCO_2/MWh)	0.97	-
$cf_{n,t}^g$	capacity factor of VRE g	-	-
α^e	percentage of baseline emissions	-	-
\bar{E}	Baseline emissions (tCO_2)	-	-

Table S7: Technical Parameters

Description	Value	Source
Specific heat capacity (kJ/kgK)	1.56	[3], [19]
Tank Insulation ($$/m^2$)	252	[19]
Tank Foundation ($$/m^2$)	1296	[19]
Hot Tank Shell Material ($$/kg$)	7.02	[19], [10]
Cold Tank Shell Material ($$/kg$)	0.59	[19], [10]
Salt Cost ($$/kg$)	1.3	[19],[10], [3]
Salt Density (kg/m^3)	1835.6	[6], [19], [3]
Hot Tank Shell Density (kg/m^3)	7959.5	[19]
Cold Tank Shell Density (kg/m^3)	7850	[19]
Shell Design Thickness (m)	0.00635	[22]
Maximum Tank Height (m)	12	[22]

Table S8: Thermal Energy Storage Characteristics

2 Integrated Dispatch and Sizing (IDS) Model Formulation

2.1 Objective Function

The objective function minimizes the sum of annualized capital cost ($CAPEX^e$), operating cost ($OPEX^e$), minus the annual revenue from grid electricity sales (REV^e). In case, we are modeling industrial heat the objective function also includes corresponding capital cost, operating cost and revenue terms for industrial process heat ($CAPEX^{ind}$, $OPEX^{ind}$, REV^{ind})

$$Z^{Obj,e} = \min(CAPEX^e + OPEX^e - REV^e) \quad (1)$$

The capital cost of TES system without heat co-production is defined in Eq. A.2 includes: 1) cost of storage, 2) cost of heat exchangers, 3) cost of resistive heaters for charging salt, 4) cost of pumps for salt flow, and 5) cost of pipes and valves that scales with discharge power capacity.

$$CAPEX^e = CRF \times (c^{TES}\Gamma + \sum_{i \in I} C^{HX,i} + c^{ht,c}Q^{ht,c} + \sum_{r=c,d} c^{p,r} + c^{pipes}\Pi^{turb}) \quad (2)$$

Here, CRF refers to the capital recovery factor is calculated based on discount rate (R) and project lifetime, which is set to be equal to the remaining lifetime of the steam cycle (L^{REM}) as $CRF = \frac{R(1+R)^{L^{REM}}}{(1+R)^{L^{REM}} - 1}$

When modeling industrial process heat, we add the following additional terms to the $CAPEX$, corresponding to the cost of the resistive heater used to directly provide process heat.

$$CAPEX^{Ind} = CRF \times c^{ht,ind} \times Q^{ht,ind} \quad (3)$$

The annual operating cost of the system is given by Eq. A.4, as the sum of fixed operating cost and variable operating cost. The variable operating cost includes the cost of power plant startups and electricity purchases from the grid during charging. Note that ω_n corresponds to the weight of representative week n , such that $\sum_{n \in N} \omega_n = 52$.

$$OPEX^e = FOM^{turbine}\bar{\Pi}^{turb} + \sum_{n \in N} \sum_{t \in T} \omega_n \times (c^{start}z_{n,t} + c_{n,t}^{elec} \times \pi_{n,t}^{net,c}) \quad (4)$$

When modeling the industrial heater, the net power consumption will include an additional term corresponding to the electricity consumption by the resistive heater providing process heat ($\sum_{n \in N} \sum_{t \in T} \omega_n \times c_{n,t}^{elec} \times \frac{1}{\eta^{ht}}q_{n,t}^{ht,c}$)

The annual operating revenues are described by Eq. A.5. When modeling heat co-production, we include an additional term equal the revenue earned from providing process heat.

$$REV^e = \sum_{n \in N} \sum_{t \in T} \omega_n \times c_{n,t}^{elec} \times \pi_{n,t}^{net,d} \quad (5)$$

2.2 Constraints

2.2.1 Net power consumption and production constraints

Net power consumption during charging is defined as power consumption by electrical heater and pumps for salt flow during charging mode.

$$\pi_{n,t}^{net,c} = \frac{1}{\eta^{ht}}q_{n,t}^{ht,c} + \pi_{n,t}^{p,c} \quad \forall t \in T, n \in N \quad (6)$$

Net power consumption during discharging is defined turbine power output minus turbine auxiliary load and salt pumping power requirements during discharging.

$$\pi_{n,t}^{net,d} = \pi_{n,t}^{turb}(1 - \epsilon^{turb}) - \pi_{n,t}^{p,d} \quad \forall t \in T, n \in N \quad (7)$$

Net power output and consumption from the facility cannot exceed existing interconnection capacity

$$\pi_{n,t}^{net,k} \leq P^{Int} \quad \forall t \in T, n \in N, k = d, c \quad (8)$$

2.2.2 Charging mode constraints

Heat supplied during charging process and associated capacity constraint.

$$q_{n,t}^{ht,c} = f_{n,t}^c \bar{C}_p \Delta T^{salt} \quad \forall t \in T, n \in N \quad (9)$$

$$q_{n,t}^{ht,c} \leq Q^{ht,c} \quad \forall t \in T, n \in N \quad (10)$$

2.2.3 Discharging mode constraints

Turbine power output at any period is less than steam cycle capacity and greater than minimum stable power output when power plant is on or zero when power is off.

$$\pi_{n,t}^{turb} \geq \beta^{min} \Pi^{turb} y_{n,t} \quad \forall n \in N, t \in T \quad (11)$$

$$\pi_{n,t}^{turb} \leq \Pi^{turb} y_{n,t} \quad \forall n \in N, t \in T \quad (12)$$

Startup constraints for steam cycle:

$$z_{n,t} \geq y_{n,t} - y_{n,t-1} \quad \forall t \in T/\{1\}, n \in N \quad (13)$$

$$z_{n,t} \geq y_{n,t} - y_{n,T} \quad \forall t = 1, n \in N \quad (14)$$

Ramping constraints for steam cycle:

$$\pi_{n,t}^{turb} - \pi_{n,t-1}^{turb} \leq \beta^{ramp,up} \Pi^{turb} \quad \forall t \in T/\{1\}, n \in N \quad (15)$$

$$\pi_{n,t}^{turb} - \pi_{n,t-1}^{turb} \geq \beta^{ramp,dn} \Pi^{turb} \quad \forall t \in T/\{1\}, n \in N \quad (16)$$

$$\pi_{n,t}^{turb} - \pi_{n,T}^{turb} \leq \beta^{ramp,up} \Pi^{turb} \quad \forall t = 1, n \in N \quad (17)$$

$$\pi_{n,t}^{turb} - \pi_{n,T}^{turb} \geq \beta^{ramp,dn} \Pi^{turb} \quad \forall t = 1, n \in N \quad (18)$$

Relating turbine power output to salt flow rate accounting for heat to power conversion efficiency.

$$\pi_{n,t}^{turb} = \eta^{turb} f_{n,t}^d \bar{C}_p \Delta T^{salt} \quad \forall t \in T, n \in N \quad (19)$$

Peak turbine capacity has to be less than available turbine capacity. Note that the steam turbine power capacity will be larger than from the nameplate capacity of the original coal power plant owing to auxiliary losses. For example, according to one estimate, auxiliary power demand at a coal power plant amounts to 5% of the steam turbine capacity implying that the power plant capacity be corresponding smaller than the steam turbine capacity.

$$\Pi^{turb} \leq \bar{\Pi}^{turb} \quad (20)$$

2.2.4 Mode Switching Constraints

Discharging (charging) salt flow rates can take non-negative values when plant is in discharging (charging) mode:

$$f_{n,t}^d \leq M y_{n,t} \quad \forall t \in T, n \in N \quad (21)$$

$$f_{n,t}^c \leq M(1 - y_{n,t}) \quad \forall t \in T, n \in N \quad (22)$$

2.2.5 Salt Pump Constraints

Pumping power requirements are proportional to salt flow rates

$$\pi_{n,t}^{p,k} = f_{n,t}^k \frac{GH}{\eta^{pump}} \quad \forall t \in T, n \in N, k = \{d, c\} \quad (23)$$

Pumping power output in each timestep cannot exceed installed pump capacity.

$$\pi_{n,t}^{p,k} \leq \Pi^{p,k} \quad \forall t \in T, n \in N, k = \{d, c\} \quad (24)$$

The cost of the pump is a linearized function of the pump power rating. m is a binary variable that enforces the cost of the pumps to be 0 when $m = 0$ and nonzero as per the linear equation when $m = 1$.

$$c^{p,k} = \Pi^{p,k} \bar{\alpha}^{p,k} + \bar{\beta}^{p,k} m \quad k = \{d, c\} \quad (25)$$

$$\Pi^{p,k} \leq m \bar{M} \quad k = \{d, c\} \quad (26)$$

2.2.6 Heat Exchanger Design Constraints

Total heat exchange across three heat exchangers must be equal to the heat delivered to steam cycle.

$$\sum_{i \in I} q_{n,t}^{hx,i} = f_{n,t}^d \bar{C}_p \Delta T^{salt} \quad \forall t \in T, n \in N \quad (27)$$

Heat exchanged via each heat exchanger cannot exceed heat exchanger design capacity.

$$q_{n,t}^{hx,i} \leq U^i A^{HX,i} \Delta T^{LM,i} \quad \forall t \in T, n \in N, i \in I \quad (28)$$

To ensure feasible heat transfer, we enforce a minimum heat exchange requirement across each heat exchanger that is computed from the Aspen simulations. Here, parameter $\beta^{hx,i}$ is such that $\sum_{i \in I} \beta^{hx,i} = 1$. This constraint ensures that each heat exchanger is utilized for heat transfer across all time peri

$$q_{n,t}^{hx,i} \geq \beta^{hx,i} \sum_{i \in I} q_{n,t}^{hx,i} \quad \forall t \in T, n \in N \quad (29)$$

Capital cost of heat exchanger is calculated as piece-wise linear approximation using the following equations. Here, $k \in K$ represent the index corresponding to various piece-wise segments.

$$\bar{C}_k^{HX,i} = \bar{C}^{HX,i} (A_k^{HX,i} / \bar{A}^{HX,i})^{\bar{n}^{HX,i}} \quad (30)$$

$$C^{HX,i} = \sum_{k \in K} \bar{C}_k^{HX,i} \lambda_k^i \quad \forall i \in I \quad (31)$$

$$A^{HX,i} = \sum_{k \in K} \bar{A}_k^{HX,i} \lambda_k^i \quad \forall i \in I \quad (32)$$

$$\sum_{k \in K} \lambda_k^i = 1 \quad \forall i \in I \quad SOS2 \quad (33)$$

2.2.7 Energy Storage Constraints

Storage energy inventory balance within a representative week is given by Eq. A.34-A.35. Note that we allow for state of charge at beginning and end of each representative week to be different by the amount, $\delta_n \in R$, a decision variable. This allows for energy to be shifted across weeks, as described further below, and thus enables long-term energy storage via TES.

$$\gamma_{n,t} = (1 - \epsilon^{sd}) \times \gamma_{n,t-1} + (f_{n,t}^c - f_{n,t}^d) \bar{C}_p \Delta T^{salt} \quad \forall n \in N, t \in T \setminus \{1\} \quad (34)$$

$$\gamma_{n,t} = (1 - \epsilon^{sd}) \times (\gamma_{n,t_{end}} - \delta_n) + (f_{n,t}^c - f_{n,t}^d) \bar{C}_p \Delta T^{salt} \quad \forall n \in N, t = 1 \quad (35)$$

Storage inventory balance across weeks of the year is modeled via the set of equations described below. Here, the net change in each storage inventory of each week is approximated by the change in storage inventory for the corresponding representative period (as per the mapping f(n)). Note that weeks are in chronological order, while representative weeks are not.

Eq. A.36 relates the storage level of the last modeled period with the storage level at the beginning of the first modeled period. If the modeled week is also a representative week, then Eq. A.38 enforces that initial storage level estimated by the intra-week storage balance constraint should equal the initial storage level estimated from the inter-week storage balance constraint.

$$s_{w+1} = (1 - \epsilon^{sd,wk}) s_w + \delta_{f(w)} \quad \forall w \in W \setminus \{w_{end}\} \quad (36)$$

$$s_1 = (1 - \epsilon^{sd,wk}) s_{w_{end}} + \delta_{f(w_{end})} \quad \forall w = w_{end} \quad (37)$$

$$s_w = \gamma_{f(w),t_{end}} - \delta_{f(w)} \quad \forall w \in W^{REP} \subset W \quad (38)$$

Eqs. A.39-A.40 enforce that initial storage level for each week and storage level during each sub-period of each representative week must be non-negative and adhere to installed energy capacity limits. The constraint in Eq. A.41 enforces that the storage inventory level in each sub-period of weeks other than representative weeks are also less than or equal to the installed capacity limit.

$$0 \leq s_w \leq \Gamma \quad \forall w \in W \quad (39)$$

$$0 \leq \gamma_{n,t} \leq \Gamma \quad \forall n \in N, t \in T \quad (40)$$

$$0 \leq s_w + \gamma_{f(w),t} - \gamma_{f(w),1} \leq \Gamma \quad \forall w \in W, t \in T \quad (41)$$

The minimum energy duration constraint is added for when we enforce the model to build a minimum amount of energy storage for \bar{h} hours.

$$\Pi^{net}\bar{h}/\eta^{turb} \leq \Gamma \quad (42)$$

2.2.8 Industrial process heat constraints

When industrial process heat supply is also modeled, the following additional constraints are added along with modifying some of the above constraints.

The constraint defining the heat supply to the steam cycle (Eq. A.43) is modified to account for heat siphoned for process heat supply:

$$\pi_{n,t}^{turb} = (f_{n,t}^d \bar{C}_p \Delta T^{salt} - q_{n,t}^{turb,ind}) \eta^{turb} \quad \forall t \in T, n \in N \quad (43)$$

Process heat supply is met via a combination of resistive heat or heat from power cycle

$$q_{n,t}^{turb,ind} + q_{n,t}^{ht,ind} = \bar{q}^{Ind} \quad \forall t \in T, n \in N \quad (44)$$

Sizing resistive heater

$$q_{n,t}^{ht,ind} \leq Q^{ht,ind} \quad \forall t \in T, n \in N \quad (45)$$

Steam from turbine can only be provided when steam cycle is operational

$$q_{n,t}^{turb,ind} \leq \bar{q}^{ind} y_{n,t} \quad \forall t \in T, n \in N \quad (46)$$

2.3 Metrics

TES Power Dispatch is defined on a yearly basis, scaled with the weighting for the representative weeks:

$$dispatch[MWh/year] = \sum_{n \in N} \sum_{t \in T} \omega_n \times \pi_{n,t}^{net,d} \quad (47)$$

Industrial Heat TES Dispatch is defined by the dispatch from the steam-turbine to the industrial demand:

$$dispatch_{ind}[MWh/year] = \sum_{n \in N} \sum_{t \in T} \omega_n \times q_{n,t}^{turb,ind} \quad (48)$$

Levelized Cost of Storage (LCOS):

$$LCOS[\$/MWh_e] = \frac{CAPEX^e + OPEX^e}{dispatch} \quad (49)$$

Duration (d):

$$d[hrs] = \frac{\eta^{turb}\Gamma}{\Pi^{net,d}} \quad (50)$$

Revenue per Dispatch (\$/MWh):

$$\frac{REV^e}{dispatch} \quad (51)$$

Industrial process heat price (p_{ind}):

$$p^{ind}[\$/MWh_t] = \frac{Z^{Obj,e} - Z^{Obj,ind}}{dispatch_{ind}} \quad (52)$$

3 Capacity Expansion Model (CEM) Formulation

The capacity expansion model (CEM) is formulated as an extension of the IDS model.

3.1 Objective Function

The objective function minimizes the sum of annualized capital cost ($CAPEX^c$) and operating cost ($OPEX^c$).

$$Z^{Obj,c} = \min(CAPEX^c + OPEX^c) \quad (53)$$

The capital cost of entire energy system is defined in Eq. A.54 includes $CAPEX^e$, the annualized cost of TES described in Eq. A.2, as well as the investment cost for Li-ion batteries, solar installations, and wind installations.

$$\begin{aligned} CAPEX^e = CRF \times & (c^{TES}\Gamma + \sum_{i \in I} C^{HX,i} + c^{ht,c}Q^{ht,c} + \sum_{r=c,d} c^{p,r} + c^{pipes}\Pi^{turb}) \\ & + \sum_{g \in G^{VRE}} c^{g,inv}\Pi^g + c^{e,inv}\Gamma^b + c^{p,inv}\Pi^b \end{aligned} \quad (54)$$

The annual operating cost of the system is given by Eq. A.55, as the sum of fixed operating cost and variable operating cost of each generator or storage device. The variable operating cost also includes the cost of power plant startups and electricity purchases from the grid during charging applied to the coal power plant and TES system. Note that ω_n corresponds to the weight of representative week n, such that $\sum_{n \in N} \omega_n = 52$.

$$\begin{aligned} OPEX^e = FOM^{turbine}\bar{\Pi}^{turb} + & \sum_{g \in G} FOM^g\Pi^g + FOM^b\Pi^b \\ & + \sum_{n \in N} \sum_{t \in T} \omega_n \times (c^{start}z_{n,t}^{TES} + c^{start}z_{n,t}^{coal} + \sum_{g \in G} OPEX^g\pi_{n,t}^g \\ & + OPEX^{dis}\pi_{n,t}^{b,d} + OPEX^{ch}\pi_{n,t}^{b,c}) \end{aligned} \quad (55)$$

3.2 Constraints

The CEM model applies constraints described by Eq A.56-A.79 to the TES system in this model.

3.2.1 Power Balance Constraints

Demand

$$d_{n,t} = \pi_{n,t}^{net,d} - \pi_{n,t}^{net,c} + \pi_{n,t}^{b,d} - \pi_{n,t}^{b,c} + \sum_{g \in G} \pi_{n,t}^g \quad \forall n \in N, t \in T \quad (56)$$

3.2.2 Emissions Constraints

Emissions

$$\sum_{n \in N} \sum_{t \in T} \omega_n \times \bar{\beta}^{coal}\pi_{n,t}^{coal} \leq \bar{\alpha}^e \bar{E} \quad (57)$$

3.2.3 Li-ion storage constraints

energy balance Initialization

$$\gamma_{n,t}^b = \gamma_{n,t-1}^b + \pi_{n,t}^{b,c}\eta^{b,c} - \pi_{n,t}^{b,d}/\eta^{b,d} - \epsilon^b\gamma_{n,t-1}^b \quad \forall t \in T/\{1\}, n \in N \quad (58)$$

Initialize

$$\gamma_{n,t}^b = (1 - \epsilon^b)\gamma_{n,T}^b + \pi_{n,t}^{b,c}\eta^{b,c} - \pi_{n,t}^{b,d}/\eta^{b,d} \quad \forall t \in \{1\}, n \in N \quad (59)$$

Sizing

$$\pi_{n,t}^{b,c} \leq \Pi^b \quad \forall t \in T, n \in N \quad (60)$$

$$\pi_{n,t}^{b,d} \leq \Pi^b \quad \forall t \in T, n \in N \quad (61)$$

$$\gamma_{n,t}^b \leq \Gamma^b \quad \forall t \in T, n \in N \quad (62)$$

3.2.4 Capacity constraints

$$\Pi^{ret} + \Pi^{coal} + \Pi^{net,d} = P^{int} \quad (63)$$

Binary exclusivity

$$x^{ret} + x^{coal} + x^{TES} = 1 \quad (64)$$

$$\Pi^{coal} \leq P^{int} x^{coal} \quad (65)$$

$$\Pi^{ret} \leq P^{int} x^{ret} \quad (66)$$

$$\Pi^{net,d} \leq P^{int} x^{TES} \quad (67)$$

$$y_{n,t}^{coal} \leq x^{coal} \quad \forall n \in N, t \in T \quad (68)$$

$$y_{n,t}^{TES} \leq x^{TES} \quad \forall n \in N, t \in T \quad (69)$$

Capacity Factor

$$\pi_{n,t}^g \leq \Pi^g c f_{n,t}^g \quad \forall n \in N, t \in T, g \in G^{VRE} \quad (70)$$

$$\pi_{n,t}^{coal} \leq \Pi^{coal} y_{n,t}^{coal} \quad \forall n \in N, t \in T \quad (71)$$

$$\pi_{n,t}^{net,d} \leq \Pi^{net,d} y_{n,t}^{TES} \quad \forall n \in N, t \in T \quad (72)$$

3.2.5 Coal Plant Constraints

ramp rates initialization

$$\pi_{n,t}^{coal} - \pi_{n,t-1}^{coal} \leq \beta^{ramp,up} \Pi^{coal} \quad \forall t \in T/\{1\}, n \in N \quad (73)$$

$$\pi_{n,t}^{coal} - \pi_{n,t-1}^{coal} \geq \beta^{ramp,dn} \Pi^{coal} \quad \forall t \in T/\{1\}, n \in N \quad (74)$$

$$\pi_{n,t}^{coal} - \pi_{n,T}^{coal} \leq \beta^{ramp,up} \Pi^{coal} \quad \forall t = 1, n \in N \quad (75)$$

$$\pi_{n,t}^{coal} - \pi_{n,T}^{coal} \geq \beta^{ramp,dn} \Pi^{coal} \quad \forall t = 1, n \in N \quad (76)$$

startup

$$z_{n,t}^{coal} \geq y_{n,t}^{coal} - y_{n,t-1}^{coal} \quad \forall t \in T/\{1\}, n \in N \quad (77)$$

$$z_{n,t}^{coal} \geq y_{n,t}^{coal} - y_{n,T}^{coal} \quad \forall t = 1, n \in N \quad (78)$$

min power

$$\pi_{n,t}^{coal} \geq \beta^{min} \Pi^{coal} y_{n,t}^{coal} \quad \forall n \in N, t \in T \quad (79)$$

3.3 Metrics

Curtailment is defined as the fraction of VRE that is not delivered to a load or stored throughout the year.

$$curtailment = 1 - \frac{\sum_{g \in G^{VRE}} \sum_{n \in N} \sum_{t \in T} \omega_n \times \pi_{n,t}^g}{\sum_{g \in G^{VRE}} \sum_{n \in N} \sum_{t \in T} \omega_n \times f_{n,t}^g \Pi^g} \quad (80)$$

System cost is the value of the objective function.

$$system\ cost = Z^{Obj,c} \quad (81)$$

4 Aspen Modeling

1) Steam turbine efficiency calculated from the coal plant simulation. $W^{HP,IP,LP}$ refers to the work from the high pressure, intermediate pressure, and low pressure turbines, W^{PUMP} is the power consumed by the water pump, and $Q^{BOILERS}$ is the heat input from the coal boilers:

$$\eta^{coal} = \frac{W^{HP} + W^{IP} + W^{LP} + W^{PUMP}}{Q^{BOILERS}} \quad (82)$$

2) Target power output of the coal plant is the rated output of the coal plant unit plus the aux power consumption. Both are reported values.

$$W^{target} = W^{rated} + W^{aux,coal} \quad (83)$$

3) We find the steam flow rate, efficiency, and other results where the power output is closest to the target power.

4) We input that steam flow rate into the TES simulation.

5) Steam Turbine Efficiency for the TES is determined from the Aspen simulations, where Q^{SALT} refers to the thermal heat input from the molten salt ($mC_P\Delta T^{Salt}$)

$$\eta^{steam} = \frac{W^{HP} + W^{IP} + W^{LP} + W^{PUMP}}{Q^{SALT}} \quad (84)$$

6) The TES calculated peak power output is the following:

$$W^{TES} = W^{HP} + W^{IP} + W^{LP} + W^{PUMP} + W^{aux,TES} \quad (85)$$

7) The interconnection capacity constraint W^{CAP} in the optimization model is either set by W^{TES} or the reported power rating of the coal plant, whichever is smaller.

5 Note on Land-Use

We conducted a back-of-envelope land use assessment with the case-study 500 MW unit and found that the land requirement for 1 to 8 GWh_t TES molten salt tanks was 1900 to 6500 square meters (which includes a 10 meter buffer). This is much less than the space available at the site, which is approximately 180,060 square meters using topical Google Maps measurements. Therefore, we do not include land availability as a constraint in the model.

6 Notes on Price Scenarios

The variability of the price profiles underpinning each price scenario affects the energy arbitrage opportunity and thus the profitability of the TES system. Table S9 below summarizes and compares the key price scenarios used in this study from 2030 [5] to the Indian Energy Exchange (IEX) average hourly market data from 2019 and 2021.

Price Scenario	Mean (\$/MWh)	std	Portion of hours less than \$5/MWh	Portion of hours greater than \$200/MWh
IEX 2019	39	11	0%	0%
IEX 2021	49	34	0%	1.5%
Maharashtra 2030	53	27	1.1 %	1.4%
Uttar Pradesh 2030	56	30	0.82%	2.15 %
Gujarat 2030	27	30	32%	0.89%
Haryana 2030	56	30	0.82%	2%
Odisha 2030	40	24	0.82%	0.85%

Table S9: Price Scenario Characteristics

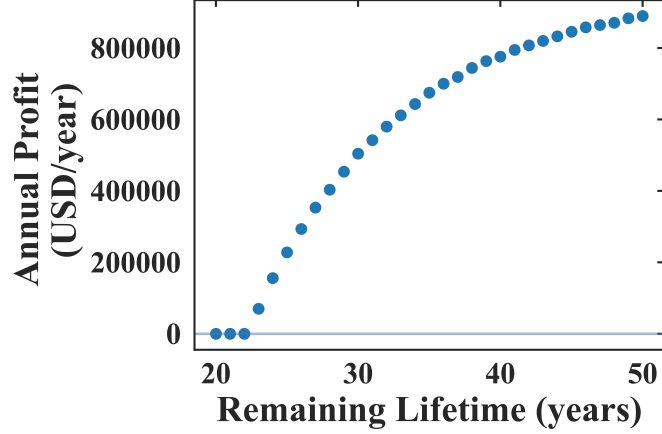


Figure S2: The remaining lifetime of the coal plant affects the annual profit. In this base case and price scenario, and without FOM, the break-even point occurs (e.g. annual profit = 0) when the remaining lifetime is 22 years.

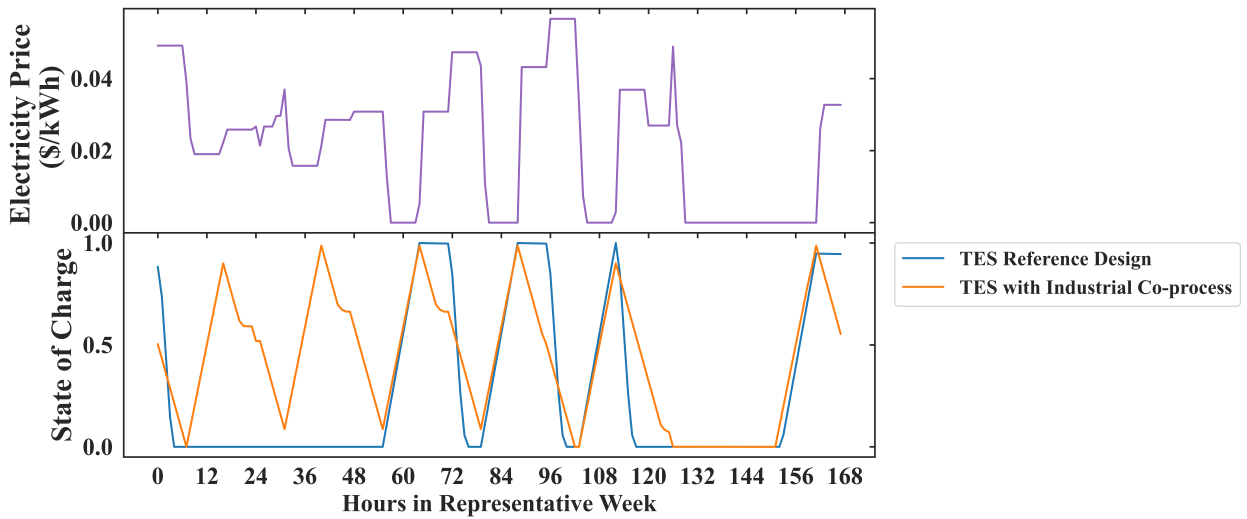


Figure S3: The TES dispatch is more sensitive to electricity price profile and exhibits more cycling under the TES design with 350 MW_t co-located industrial process heat supplied at a constant 180°C compared to the the base stand-alone TES system design under the 2030 Gujarat price scenario. TES could technically serve lower industrial heat demands and assist in industrial decarbonization efforts particularly in industrial parks with high percentages of captive coal units. It is an economically viable method when compared to using electric resistive heaters to supply the heat load, but the ultimate economic viability of such a system depends on site-specific decisions.

7 Supporting Figures

```
mystyle backgroundcolor=CadetBlue!15!white, commentstyle=Red3, numberstyle=gray, stringstyle=Blue3, basicstyle=,
breakatwhitespace=false, breaklines=true, numbers=left, numbersep=5pt, showspaces=false, showstringspaces=false,
showtabs=false, tabsize=2 language=[5.3]Lua,style=mystyle
```

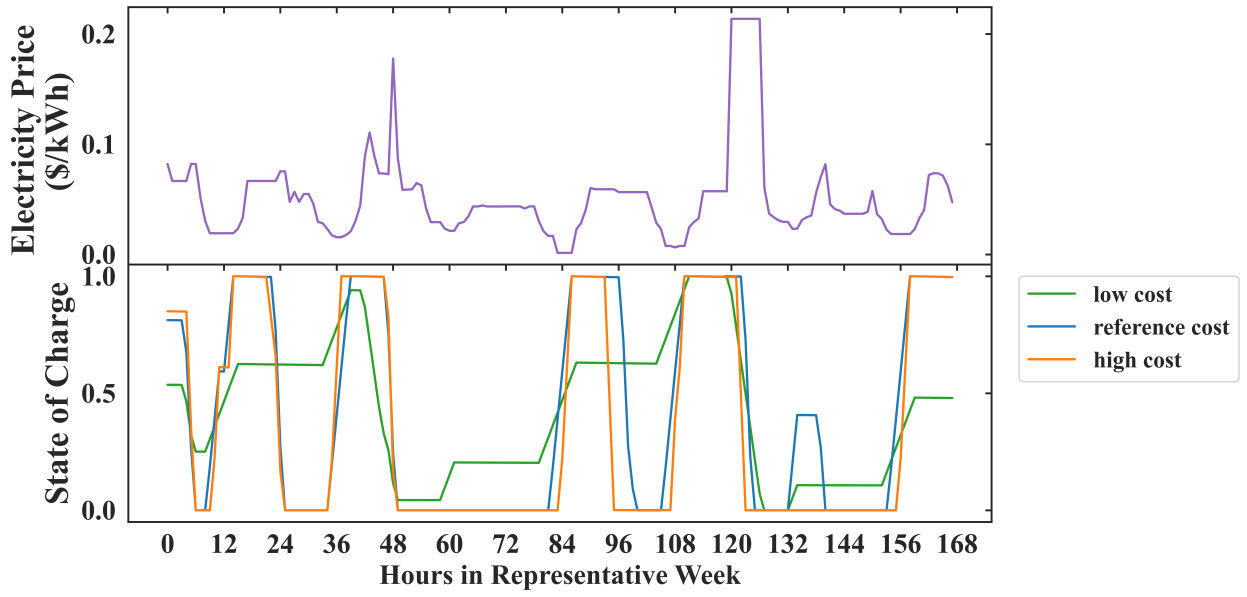


Figure S4: The TES dispatch is sensitive to storage costs. The lowest cost storage ($\$4/\text{kWh}$) cycles more often than the reference cost ($\$21/\text{kWh}$) and high cost ($\$41/\text{kWh}$).

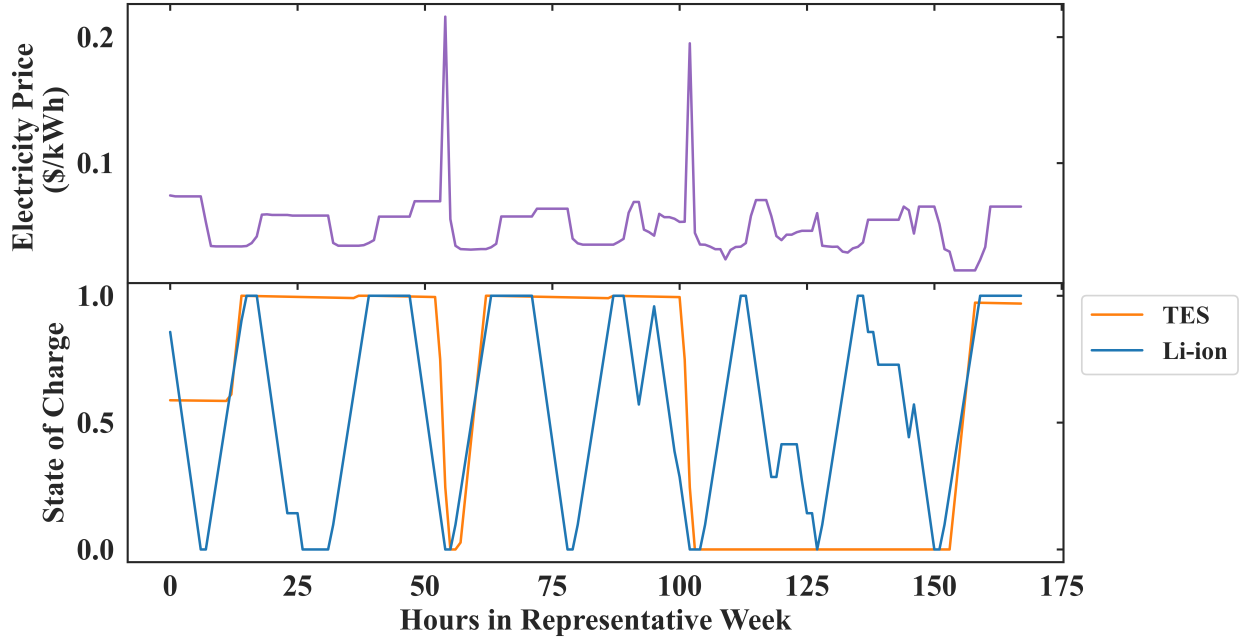


Figure S5: Li-ion dispatch shows more cycling and sensitivity to the price profile compared to TES dispatch which exhibits a longer, weekly cycle. Li-ion assumptions include: investment costs ($\$49/\text{kW}$ per year and $\$17/\text{kWh}$ per year), FOM ($\$6/\text{MW/year}$), OPEX ($\$0.1/\text{MWh}$), charging and discharging efficiency (0.95). In this result with a 2 hour minimum build enforced, the Li-ion cost is $\$110/\text{MWh}$ and TES is $\$242/\text{MWh}$.

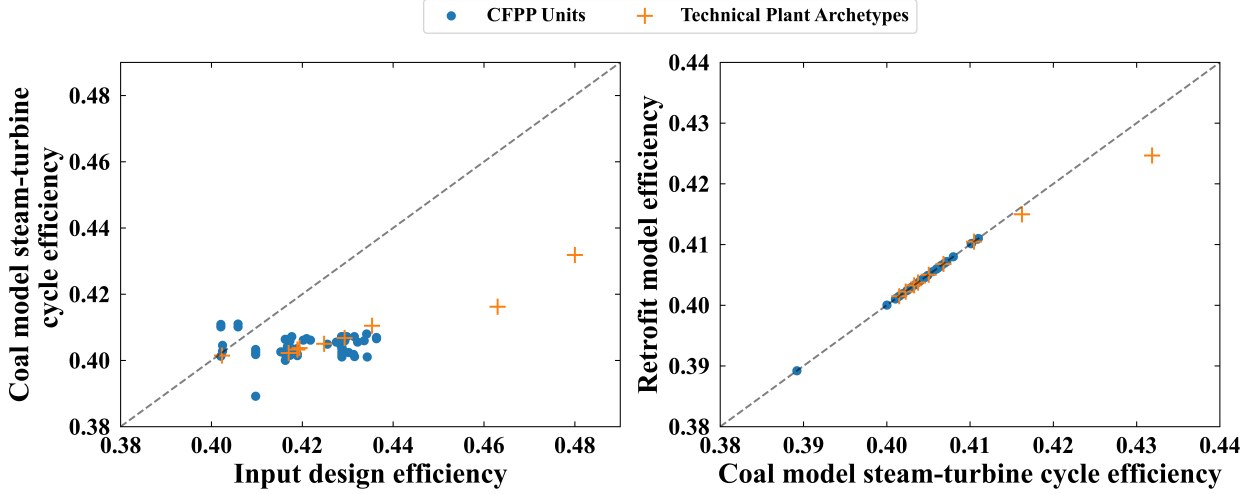


Figure S6: The left plot shows that the coal plant model in Aspen is calibrated to the input design efficiency of the steam turbine as reported, but the model often does not reach the same design steam turbine efficiency under the practical design limits imposed. This serves as a lower bounded value for efficiency. The right plot shows the coal model steam turbine efficiency calibrating the thermal energy storage retrofit discharge efficiency for the same units.

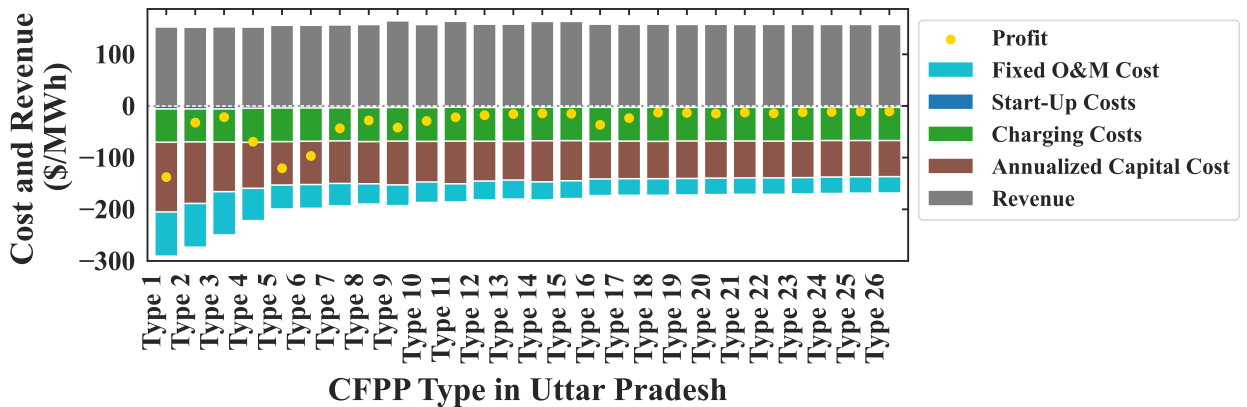


Figure S7: Levelized Cost of Storage (LCOS) values for each representative group of CFPP unit in Uttar Pradesh. These groups were determined by grouping capacity and age of each unit and assigning them to the appropriate cluster. This LCOS graphic shows main drivers of cost, namely the charging costs, capital costs, and the Fixed O&M costs. Revenue per dispatch is also plotted, and overlaid with annual profit per dispatch (which is the simple difference between the LCOS and revenue). Under this assumed Fixed O&M, 0% of the fleet is profitable under the 2030 Uttar Pradesh electricity price scenario.

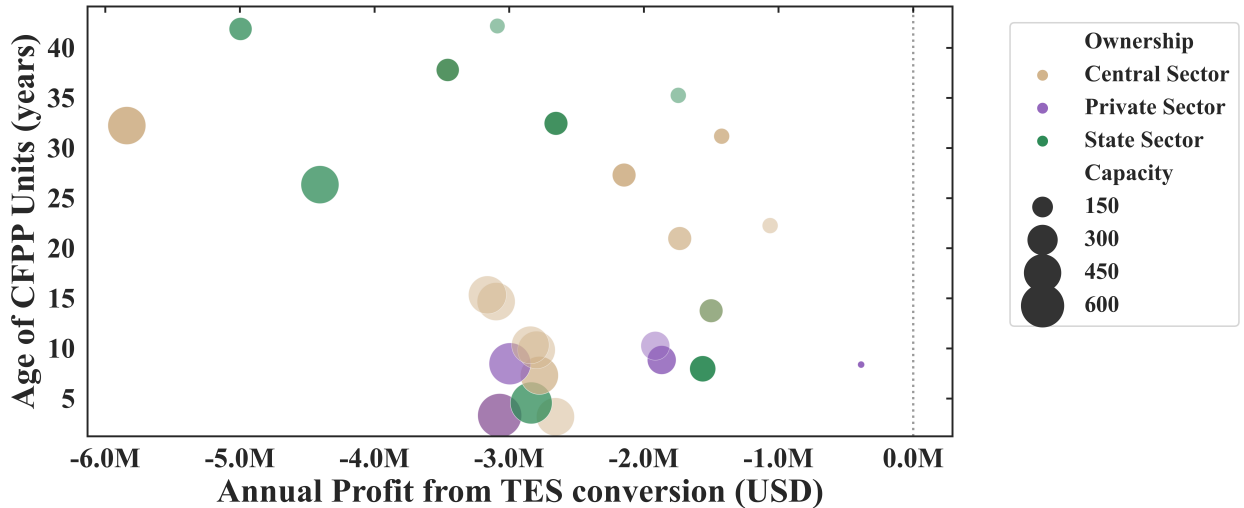


Figure S8: Annual profit or loss from IDS for each CFPP in Uttar Pradesh, based on the 26 representative units classified by age and capacity. Under this assumed Fixed O&M, 0% of the fleet is profitable under the 2030 Uttar Pradesh electricity price scenario.

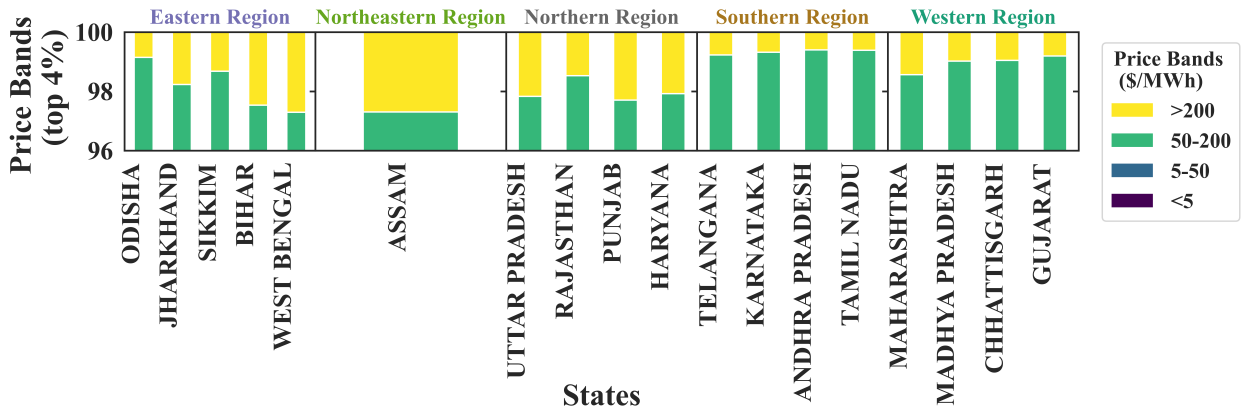


Figure S9: This plot shows the top 4% of electricity prices per price profile. The bands are grouped into bins of above \$200/MWh and between \$50 and \$200/MWh. The price profiles are the input to the integrated dispatch and optimization model and are made of 23 representative weeks derived from a k-means clustering analysis from the original year-long hourly profile per state.

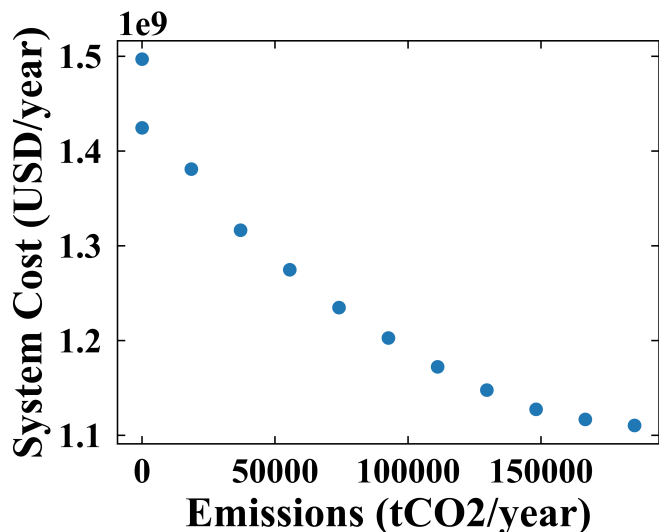


Figure S10: System emissions and system cost trade-off

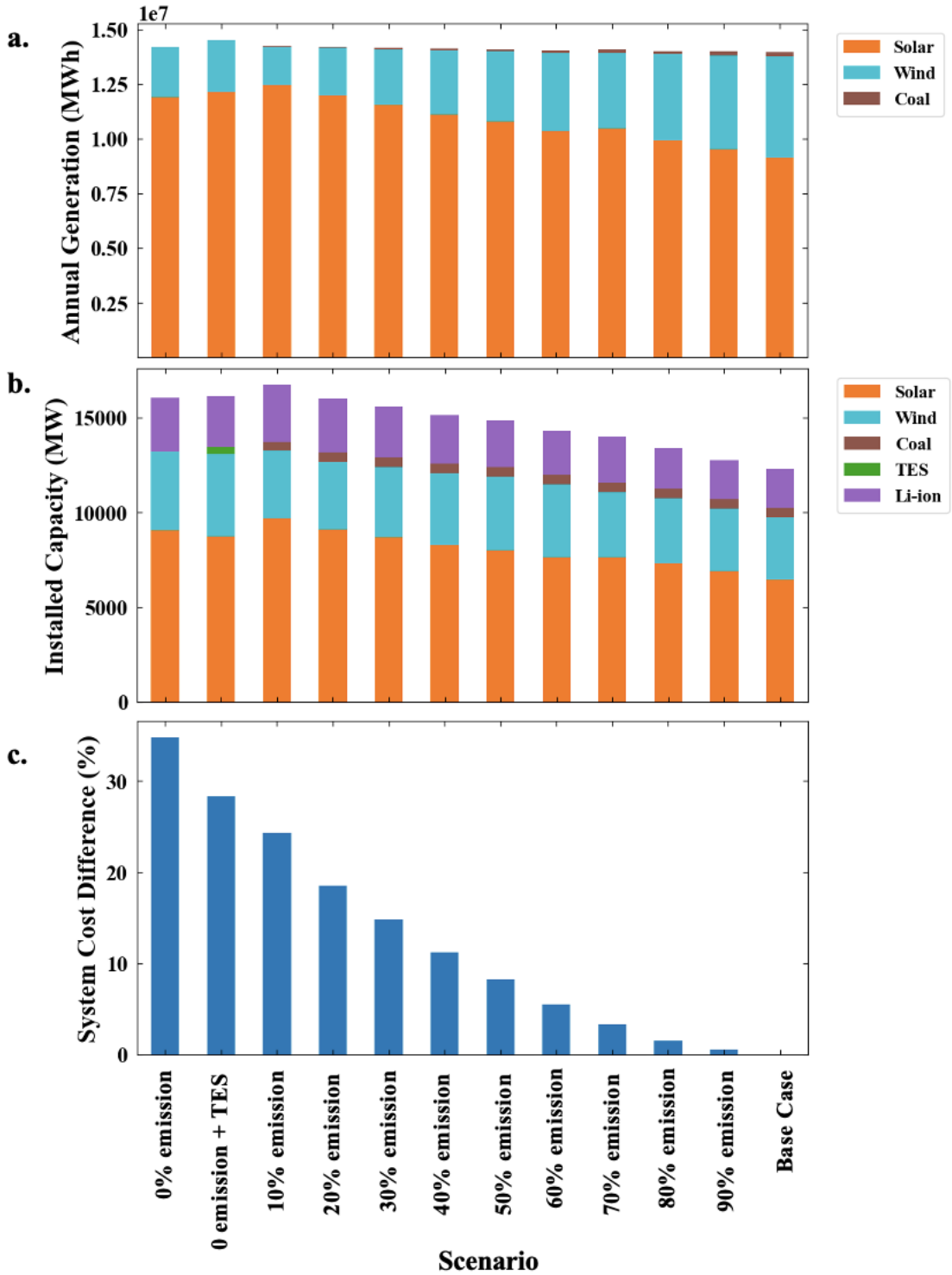


Figure S11: **a.** Annual Generation (MWh), **b.** Installed Capacity (MW), and **c.** System Cost Difference for Scenarios with emissions constraints. With more stringent emissions constraints, the coal plant capacity factor decreases (as seen in the annual generation plot), the amount of VRE + storage capacity installed increases, and the system cost generally increases from the base case. TES retrofits is optimal to deploy in the zero emissions case, and results in lower system costs than the zero emissions case without TES that simply retires coal. Both zero emissions cases do not have any installed coal capacity.

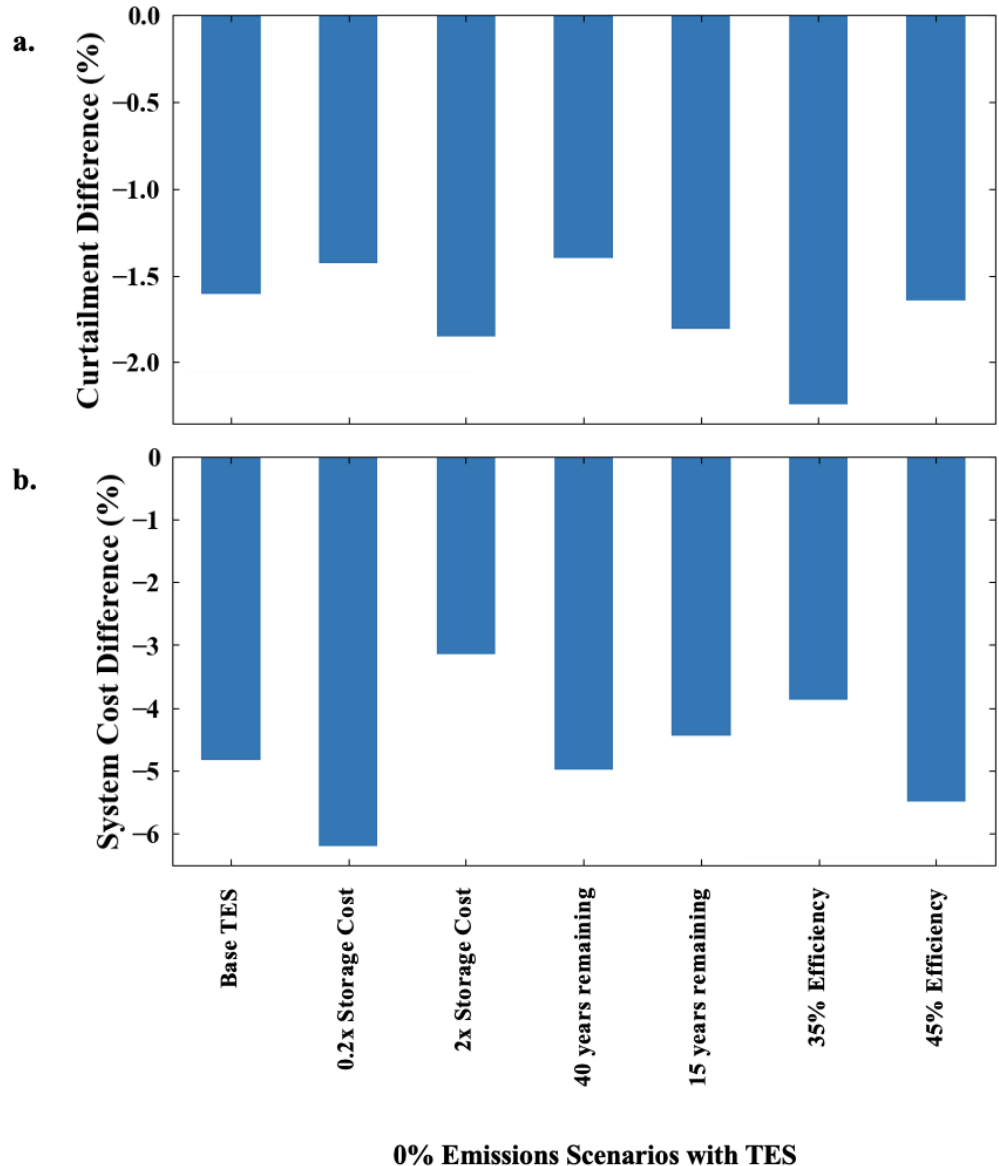


Figure S12: For the zero-emissions cases, this figure compares the percentage reduction in **a.** curtailment and **b.** system cost from the zero-emissions case with no option to deploy TES retrofits and full coal retirement is the only option. The sensitivities compared exhibit similar trends to the plant-level modeling sensitivities and include: TES storage capacity cost, years remaining, and steam-turbine efficiency, with the storage and efficiency causing the largest range of impacts on system cost.

References

- [1] Central Electricity Agency. First indian technology catalogue. 2022.
- [2] Marc Barbar, Dharik S Mallapragada, Meia Alsup, and Robert Stoner. OPEN Scenarios of future Indian Data Descriptor electricity demand accounting for space cooling and electric vehicle adoption. *Scientific Data*, page 12.
- [3] Adrián Caraballo, Santos Galán-Casado, Ángel Caballero, and Sara Serena. Molten Salts for Sensible Thermal Energy Storage: A Review and an Energy Performance Analysis. *Energies*, 14(4):1197, February 2021.
- [4] Castalia. The Role of Concentrated Solar Power in the Power System of the Future, July 2021.
- [5] Ilya Chernyakhovskiy, Mohit Joshi, David Palchak, and Amy Rose. Energy Storage in South Asia: Understanding the Role of Grid-Connected Energy Storage in South Asia's Power Sector Transformation. Technical Report NREL/TP-5C00-79915, 1811299, MainId:39133, July 2021.
- [6] Wenjin Ding, Hao Shi, Yanlei Xiu, Alexander Bonk, Alfons Weisenburger, Adrian Jianu, and Thomas Bauer. Hot corrosion behavior of commercial alloys in thermal energy storage material of molten MgCl₂/KCl/NaCl under inert atmosphere. *Solar Energy Materials and Solar Cells*, 184:22–30, September 2018.
- [7] Trading Economics. Inflation CPI. Accessed Online.
- [8] Cristina Elsido, Emanuele Martelli, and Ignacio E. Grossmann. Multiperiod optimization of heat exchanger networks with integrated thermodynamic cycles and thermal storages. *Computers & Chemical Engineering*, 149:107293, June 2021.
- [9] Karthik Ganesan and Danwant Narayanaswamy. Variable Cost, Efficiency and Financial Solvency. page 58.
- [10] Greg Glatzmaier. Developing a Cost Model and Methodology to Estimate Capital Costs for Thermal Energy Storage. Technical Report NREL/TP-5500-53066, 1031953, December 2011.
- [11] Mei Gong and Fredric Ottermo. High-temperature thermal storage in combined heat and power plants. *Energy*, 252:124057, August 2022.
- [12] P.A. González-Gómez, J. Gómez-Hernández, J.V. Briongos, and D. Santana. Thermo-economic optimization of molten salt steam generators. *Energy Conversion and Management*, 146:228–243, August 2017.
- [13] William T. Hamilton, Mark A. Husted, Alexandra M. Newman, Robert J. Braun, and Michael J. Wagner. Dispatch optimization of concentrating solar power with utility-scale photovoltaics. *Optim Eng*, 21(1):335–369, March 2020.
- [14] Indo-German Energy Program (IGEN). Mapping of 85 pulverized coal fired thermal power generating units in different states.
- [15] Mitsubishi Heavy Industries. Tandem Steam Turbine for Cogeneration Power Plant (Optimization for Min. Load Operation), 2007.
- [16] MIT Energy Initiative. The Future of Energy Storage, May 2022.
- [17] Robert James, III, Dale Keairns, Marc Turner, Mark Woods, Norma Kuehn, and Alex Zoelle. Cost and Performance Baseline for Fossil Energy Plants Volume 1: Bituminous Coal and Natural Gas to Electricity. Technical Report NETL-PUB-22638, 1569246, September 2019.
- [18] Nikil Kumar, Philip Besuner, Steven Lefton, Dwight Agan, and Douglas Hilleman. Power Plant Cycling Costs. Technical Report NREL/SR-5500-55433, 1046269, July 2012.
- [19] Ming Liu, N.H. Steven Tay, Stuart Bell, Martin Belusko, Rhys Jacob, Geoffrey Will, Wasim Saman, and Frank Bruno. Review on concentrating solar power plants and new developments in high temperature thermal energy storage technologies. *Renewable and Sustainable Energy Reviews*, 53:1411–1432, January 2016.
- [20] Aspen Plus. <https://www.aspentechn.com/en/products/engineering/aspen-plus>.
- [21] Kevin R. Robb, Prashant K. Jain, and Thomas J. Hazelwood. High-Temperature Salt Pump Review and Guidelines - Phase I Report. Technical Report ORNL/TM-2016/199, 1257909, May 2016.
- [22] Samaan Ladkany, William Culbreth, and Nathan Loyd. Molten Salts and Applications II: 565 °C Molten Salt Solar Energy Storage Design, Corrosion, and Insulation. *JEPE*, 12(11), November 2018.